
Proceedings Paper:
Dantas, R., Correia, J., Lesiuk, G. et al. (5 more authors) (2020) Multiaxial fatigue assessment of S355 steel in the high-cycle region by using Susmel's criterion. In: Iacoviello, F., Sedmak, A., Marsavina, L., Blackman, B., Ferro, G.A., Shlyannikov, V., Ståhle, P., Zhang, Z., Moreira, P.M.G.P., Božic, Z. and Banks-Sills, L., (eds.) Procedia Structural Integrity. 1st Virtual European Conference on Fracture - VECF1, 29 Jun - 01 Jul 2020, Online. Elsevier , pp. 796-803.

https://doi.org/10.1016/j.prostr.2020.10.093

Available online at www.sciencedirect.com

ScienceDirect

Procedia Structural Integrity 28 (2020) 796–803

Structural Integrity Procedia

www.elsevier.com/locate/procedia

1st Virtual European Conference on Fracture

Multiaxial fatigue assessment of S355 steel in the high-cycle region by using Susmel's criterion

Rita Dantas[a*], José Correia[a], Grzegorz Lesiuk[b], Dariusz Rozumek[c], Shun-Peng Zhu[d], Abílio de Jesus[a], Luca Susmel[e] and Filippo Berto[f]

[a]*Faculty of Engineering of the University of Porto, Rua Roberto Frias, Porto, 4200-465, Portugal*
[b] *Faculty of Mechanical Engineering, Wrocław University of Science and Technology, Smoluchowskiego 25, Wrocław, 50-370, Poland*
[c]*Opole University of Technology, Mikołajczyka 5, Opole, 45-271, Poland*
[d]*School of Mechanical and Electrical Engineering, University of Electronic Science and Technology of China, Chengdu 611731, China*
[e]*Department of Civil and Structural Engineering, University of Sheffield, Mappin Street, Sheffield, S1 3JD, England*
[f]*Department of Mechanical and Industrial Engineering, NTNU – Norwegian University of Science and Technology, Trondheim, Norway*

Abstract

Multiaxial fatigue is frequently present on engineering structures and is the cause of many mechanical failures. However, multiaxial fatigue analysis is full of questions and different points of view. Thus, throughout this study, Susmel's criterion, a recent multiaxial fatigue damage model also known as the Modified Wöhler Curve Method, is presented, explained and assessed. Experimental data of axial, torsional and proportional (axial+torsional) fatigue tests conducted on S355 structural steel and under different stress ratios were analysed and evaluated according to this model. Mean fatigue design curves for each loading condition were obtained and plotted in the high cycle fatigue region. Finally, the ability of Susmel's criterion to assess the multiaxial fatigue behaviour of S355 steel in the high cycle region was evaluated by determining the error index between the theoretically estimated and the experimental fatigue damage. Susmel's model was found to be adequate to describe the fatigue behaviour of the steel under study in high cycle region.

Keywords: multiaxial fatigue; susmel model; structural steel; high cycle fatigue

* Corresponding author.
E-mail address: up201403351@fe.up.pt

10.1016/j.prostr.2020.10.093

Nomenclature

τ_a	maximum shear stress on the critical plane
N_f	number of cycles to failure
N_{ref}	reference number of cycles to failure
$\tau_{a,ref}$	endurance limit at N_{ref}
k_τ	negative inverse slope of the modified Wöhler curve
ρ_{eff}	effective value of the critical plane stress ratio
$\sigma_{n,m}$	normal mean stress to the critical plane
$\sigma_{n,a}$	normal stress amplitude to the critical plane
m	mean stress sensitivity index
R	stress ratio
$\tau_a^*, \sigma_{n,m}^*, \sigma_{n,a}^*$	shear and normal stress components to the critical plane of an endurance limit with R>-1
$N_{f,e}$	estimated number of cycles to failure
α, β, a, b	material fatigue constants
σ_a	endurance limit for fully reversed uniaxial loading
$\tau_{a,0}$	endurance limit for fully reversed torsional loading
k	negative inverse slope of the fully reversed uniaxial loading modified Wöhler curve
k_0	negative inverse slope of the fully reversed torsional loading modified Wöhler curve
ρ_{lim}	limit value of ρ_{eff}
f_u	tensile strength
f_y	yield strength
E	young modulus
μ	mean
σ	standard deviation

1. Introduction

Fatigue is a critical degradation process affecting engineering structures and it is believed to be responsible for half of the failures of mechanical components. In particular, multiaxial fatigue is frequently observed in engineering applications, such as wind turbines or offshore structures, not only due to complex loading scenarios, but also due to notches and geometries that originate a multiaxial stress state in the presence of uniaxial loadings (Kamal & Rahman, 2018).

Therefore, around the middle of the twentieth century, a couple of different models and approaches which aimed at addressing the multiaxial fatigue problem were developed and studied such as the models presented by Gough and Pollard, Findley, Sines and Matake (Findley, 1958; Gough & Pollard, 1935; Matake, 1977; Sadek & Olsson, 2016; Sines, 1955, 1959). Nowadays, in spite of these models' wide and spread application, new ones have been formulated and multiaxial fatigue remains an open topic. Some of these new modern models are: Dang Van's multi-scale approach, which proposes a model based on the interaction between macroscopic and mesoscopic scales, Papadopoulos' and Carpinteri-Spagnoli's models, which propose complex approaches for hard metals, and Susmel's model, which will be presented throughout this work (Carpinteri & Spagnoli, 2001; Dang-van, 1993; I. V. Papadopoulos, 1994).

Hence, this work aims at comprehending and evaluating the ability of Susmel's model to assess the fatigue behavior of S355 steel in high-cycle fatigue region and under proportional loading. Therefore, experimental fatigue data from previous researches were re-analysed and used to assess this multiaxial fatigue model under study as well as to determine fatigue design curves for each loading condition. Finally, the index errors between experimental and theoretical fatigue damage were calculated and analysed. This assessment has focused on proportional loading with constant amplitude, so that material mechanisms related to more complex loadings, such as non-proportional or variable amplitude, will be left for future researches and works.

2. Overview on Susmel Model

In the last years, Susmel has developed and proposed a multiaxial fatigue model which is a critical plane approach based on a Modified Wöhler Curve (L. Susmel, 2008; L. Susmel & Lazzarin, 2002). This model relies on the assumption that, under constant loading, fatigue damage and the probability of initiating a crack reach their maximum value on the material plane that experiences the maximum shear stress amplitude. This plane is called the critical plane (L. Susmel, 2008, 2009; L. Susmel & Lazzarin, 2002; L. Susmel & Tovo, 2011; L Susmel, 2013; L Susmel, Hattingh, James, & Tovo, 2017; Luca Susmel, 2010).

Hence, the damage assessment of this model is summarized via a modified Wöhler diagram, which plots the maximum shear stress on the critical plane (τ_a) as a function of the number of cycles to failure (N_f) (Fig. 1). The design curves of this diagram are defined by two different variables: the negative inverse slope (k_τ) and the endurance limit ($\tau_{a,ref}$) at a certain established number of cycles to failure (N_{ref}). Both variables mentioned are characterized by a third variable: the effective value of the critical plane stress ratio (ρ_{eff}), which is given by the following equation:

$$\rho_{eff} = \frac{m \cdot \sigma_{n,m} + \sigma_{n,a}}{\tau_a} \tag{1}$$

where $\sigma_{n,m}$ is the normal mean stress, $\sigma_{n,a}$ is the normal stress amplitude, both stresses relative to the critical plane, and m is the mean stress sensitivity index and a material property, which varies between 0 and 1 (L. Susmel, 2010). Index m can be calculated through the equation bellow:

$$m = \frac{\tau_a^*}{\sigma_{n,m}^*}\left(2\frac{\tau_{a,R=-1} - \tau_a^*}{2\tau_{a,R=-1} - \sigma_{a,R=-1}} - \frac{\sigma_{n,a}^*}{\tau_a^*}\right) \tag{2}$$

where τ_a^*, $\sigma_{n,m}^*$ and $\sigma_{n,a}^*$ are the shear stress amplitude, the normal mean stress amplitude and the stress amplitude to the critical plane for a fatigue limit with a stress ratio (R) larger than -1, while $\tau_{a,R=-1}$ and $\sigma_{a,R=-1}$ are the fully reversed endurance limits for uniaxial and torsional loading cases. Therefore, with the aim of determining this material constant, three different endurance limits should be known and, when they are not, the material under study is considered as fully sensitive to normal mean stress and, consequently, m is assumed to be equal to 1 (L. Susmel, 2009).

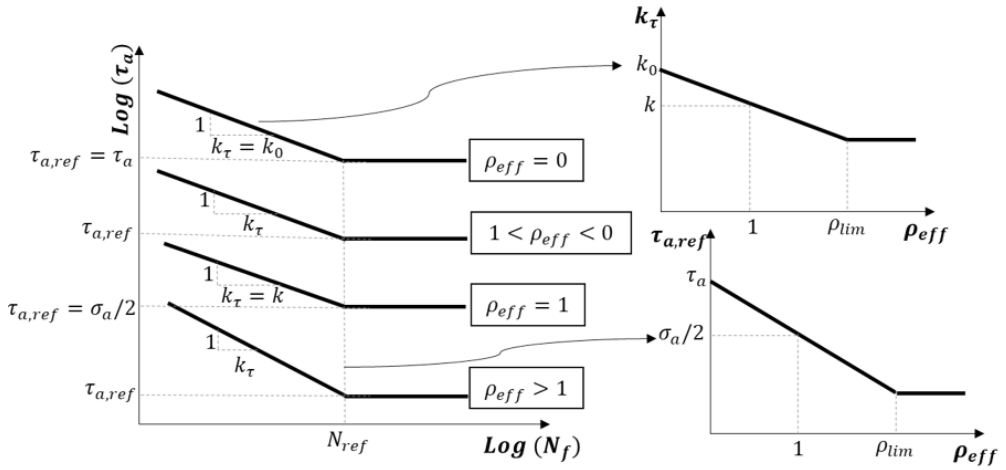

Fig. 1 Scheme of Susmel's model variables and plots: modified Wöhler diagram (left), k_τ vs ρ_{eff} (right top) and $\tau_{a,ref}$ vs ρ_{eff} (right bottom)

As it is portrayed in Fig. 1, there is one single design curve for each loading scenario associated with the corresponding ρ_{eff} value which, as mentioned above, originates also different pairs of $\tau_{a,ref}$ and k_τ values, that characterize each curve. Thus, these curves are defined by the following equation, which gives the estimated number of cycles to failure ($N_{f,e}$):

$$N_{f,e} = N_{Ref} \cdot \left[\frac{\tau_{a,ref}(\rho_{eff})}{\tau_a}\right]^{k_\tau(\rho_{eff})} \quad (3)$$

As can be observed from Eqs. (1) and (3), ratio ρ_{eff} plays a significant role in fatigue life estimation and portrays the non-zero mean stresses, the degree of multiaxiality and the non-proportionality of the loading history. Furthermore, this ratio is always equal to unity under fully-reversed uniaxial fatigue loading and equal to zero under fully-reversed torsional fatigue loading. These two loading scenarios are usually used to calibrate the model (L Susmel et al., 2017).

Lastly, variables k_τ and $\tau_{a,ref}$ can be determined through the following equations:

$$k_\tau(\rho_{eff}) = \alpha \cdot \rho_{eff} + \beta \quad (4)$$

$$\tau_{a,ref}(\rho_{eff}) = a \cdot \rho_{eff} + b \quad (5)$$

where α, β, a and b are material fatigue constants, which can be determined through the fatigue curves of fully reversed uniaxial ($\rho_{eff} = 1$; $k_\tau(\rho_{eff} = 1) = k$; $\tau_{a,ref}(\rho_{eff} = 1) = \sigma_a/2$) and torsional ($\rho_{eff} = 0$; $k_\tau(\rho_{eff} = 0) = k_0$; $\tau_{a,ref}(\rho_{eff} = 0) = \tau_{a,0}$) loadings that are usually well-known or easily to experimentally determine. Thus, Equations (4) and (5) can be rewritten as:

$$k_\tau(\rho_{eff}) = (k - k_0)\rho_{eff} + k_0, \text{ for } \rho_{eff} \leq \rho_{lim} \quad (6)$$

$$k_\tau(\rho_{eff}) = (k - k_0)\rho_{lim} + k_0, \text{ for } \rho_{eff} > \rho_{lim} \quad (7)$$

$$\tau_{a,ref}(\rho_{eff}) = \left(\frac{\sigma_a}{2} - \tau_{a,0}\right)\rho_{eff} + \tau_{a,0} = const., \text{ for } \rho_{eff} \leq \rho_{lim} \quad (8)$$

$$\tau_{a,ref}(\rho_{eff}) = \left(\frac{\sigma_a}{2} - \tau_{a,0}\right)\rho_{lim} + \tau_{a,0} = const., \text{ for } \rho_{eff} > \rho_{lim} \quad (9)$$

where ρ_{lim} is a limit value imposed to ρ_{eff}, since Susmel's model becomes conservative for high values of ρ_{eff}, and it can be determined through the application of the equation bellow (L. Susmel, 2008):

$$\rho_{lim} = \frac{\tau_{a,0}}{2\tau_{a,0} - \sigma_a} \quad (10)$$

3. Experimental Data

In order to analyse the fatigue behaviour of S355 steel as well as evaluate the accuracy of Susmel's model to describe it, experimental data already obtained and determined in previous works were analysed (R. Dantas et al., 2019; Rita Dantas, 2019; Rozumek & Pawliczek, 2004). These experimental data were determined by performing uniaxial, torsional and biaxial (torsional+axial) fatigue tests on smooth hourglass specimens of S355 structural steel (young modulus: $E = 211.6MPa$; yield strength: $f_y = 367MPa$; tensile strength: $f_u = 579MPa$; hardness=$151.28HV10$) (Correia, de Jesus, Fernández-Canteli, & Calçada, 2015). In sum, forty-four experimental fatigue points were analysed throughout this work.

For uniaxial and biaxial loading conditions experimental data were available for two different stress ratios, i.e.: R=0.01 and R=-1, while the experimental fatigue data for torsional loading were generated solely under fully-reversed loading. Furthermore, in the biaxial fatigue tests the shear stress and the normal stress were in-phase and the first one was defined as half of the second one. Another important aspect to mention is that all fatigue tests being considered were performed in order to evaluate the strength of this material in the high-cycle region (between $5 \cdot 10^4$ and $5 \cdot 10^6$ cycles) and with constant amplitude loading.

4. Multiaxial Fatigue Model Application and Results

The first step to apply Susmel's method implies rewriting Eq. (3), in order to obtain a general function which defines and describes the different design curves for each loading, as can be found bellow:

$$\tau_a = \tau_{a,ref}\left(\rho_{eff}\right)\left(\frac{N_f}{N_{ref}}\right)^{-\frac{1}{k_\tau\left(\rho_{eff}\right)}} \tag{11}$$

In the above equation, there are four unknown variables which have to be calculated: $\tau_{a,ref}$, k_τ, ρ_{eff} and N_{ref}. Following the procedure present by Susmel, N_{ref} was taken equal to $2 \cdot 10^6$ cycles, index m was determined to be equal to 0.31 (Eq. (2)) and, then, the different values of ρ_{eff} for each loading case were calculated through Eq. (1) (Table 1) (L. Susmel, 2009).

Table 1. Values of ρ_{eff} for each loading condition under study

Loading Condition	R	ρ_{eff}
Axial	0.01	1.32
Axial	-1	1
Axial+Torsional ($\sigma = 2\tau$)	0.01	0.93
Axial+Torsional ($\sigma = 2\tau$)	-1	0.7
Torsional	-1	0

Regarding ρ_{eff}, it is also important to determine the limit value (ρ_{lim}), which was calculated through Eq. (10) to be equal to 1.36. At this point, the model was calibrated, i.e., in other words, constants a, b, α and β in Eqs. (6)-(9) were determined using the values for $\tau_{a,ref}$ and k_τ for the fully reversed uniaxial and torsional loading cases as well as the already known values for ρ_{eff}, which are always 0 and 1 for these particular loading conditions, not being influenced by the value of m. Thus, the modified Wöhler diagrams, which plot τ_a versus N_f, for both loading conditions were obtained through a simple non-linear regression of the experimental fatigue data and consequently $\tau_{a,ref}$ and k_τ were calculated. Therefore, constants a, b, α and β were calculated and the linear functions which define the values of $\tau_{a,reff}$ and k_τ for each value of ρ_{eff} were determined as:

$$k_\tau = 7.8\rho_{eff} + 10.4 \tag{12}$$

$$\tau_{a,ref} = -67\rho_{eff} + 183 \tag{13}$$

After that, the different values for $\boldsymbol{k_\tau}$ and $\boldsymbol{\tau_{a,ref}}$ for each loading condition were calculated as well as the design curves according to Susmel's model, which for torsional loading with R=-1, axial loading with R=0.01, axial loading with R=-1, proportional loading with R=0.01 and proportional loading with R=-1, are defined by the following equations, respectively:

$$\tau_a = 183\left(\frac{N_f}{2{\cdot}10^6}\right)^{-0.096} \tag{14}$$

$$\tau_a = 95\left(\frac{N_f}{2{\cdot}10^6}\right)^{-0.048} \tag{15}$$

$$\tau_a = 116\left(\frac{N_f}{2{\cdot}10^6}\right)^{-0.055} \tag{16}$$

$$\tau_a = 121\left(\frac{N_f}{2\cdot 10^6}\right)^{-0.057} \tag{17}$$

$$\tau_a = 136\left(\frac{N_f}{2\cdot 10^6}\right)^{-0.063} \tag{18}$$

All the fatigue design curves calculated and the corresponding experimental data are plotted in a single modified Wöhler diagram and can be seen in Fig. 2.

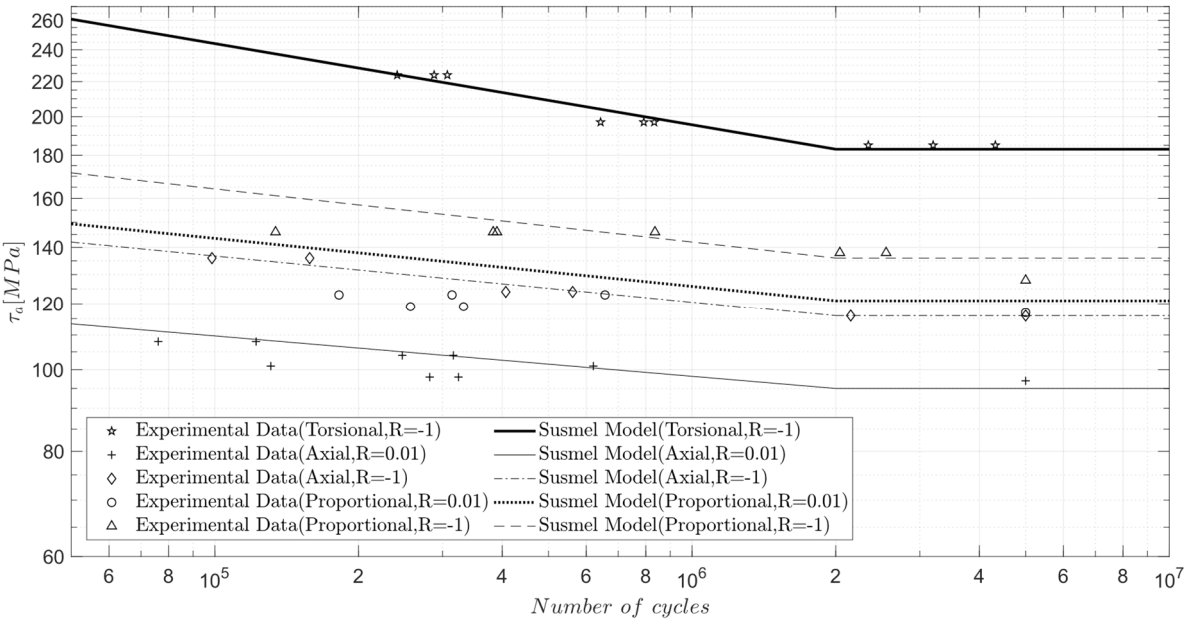

Fig. 2. Fatigue design curves determined using Susmel Model for different loading conditions

In order to evaluate the accuracy of this method, it was calculated the error index which quantifies the deviation between the estimated fatigue damage and the experimental fatigue damage observed at a certain number of cycles, by applying the following equation (Ioanis V. Papadopoulos, Davoli, Gorla, Filippini, & Bernasconi, 1997; Zhang, Shang, Sun, & Wang, 2018):

$$error\ index_i\ (\%) = \frac{experimental\ value - theoretical\ value}{theoretical\ value}\cdot 100\%, i = specimen\ number \tag{19}$$

Furthermore, it was assumed that the error index calculated for each specimen could be treated as a random variable, following a normal distribution with a f probability density function characterized by a mean value (μ) and a standard deviation (σ). Afterwards, a histogram of frequencies was plotted with the error indexes calculated and the probability density function was also plotted in the same graph. As can be seen in Fig. 3 (a), the values of error index are mainly around 0% and 5% as well as the mean value is bellow 5%, which shows that Susmel's model is highly accurate in describing the fatigue behavior of S355 steel. These low values of index errors are emphasized and confirmed by the graph of Fig. 3 (b) which plots the theoretical number of cycles calculated by Susmel's model versus the experimental number of cycles.

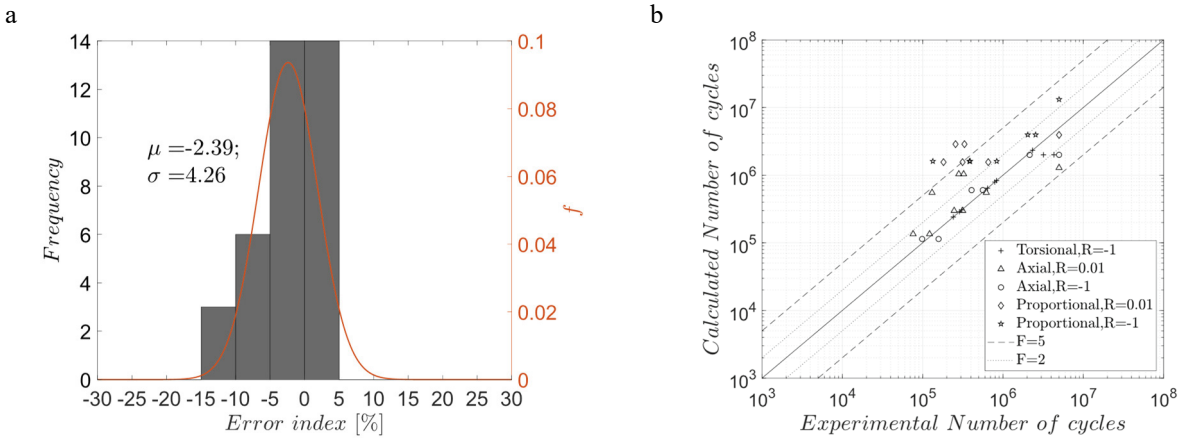

Fig. 3 (a) Frequency histograms and density functions of the normal distribution of the error index (b) Calculated number of cycles versus experimental number of cycles until failure graph

5. Conclusions

Throughout this research work, axial, torsional and proportional (axial and torsional) experimental fatigue data for S355 steel tested, under a stress ratio equal to 0 and -1, in the high-cycle region were analysed and studied. Susmel's model was reviewed, explained and applied to post-process the experimental data being considered. Afterwards, mean fatigue design curves for each kind of loading were determined and plotted according to Susmel's model. Subsequently, it was concluded that Susmel's model is markedly accurate in modelling and assessing multiaxial high cycle fatigue damage in S355 steel subjected to different loading conditions.

In the future, a probabilistic analysis will be performed, and a probabilistic design curve will be determined in order to complete this study.

Acknowledgements

This work was supported by base funding - UIDB/04708/2020 and programmatic funding - UIDP/04708/2020 of the CONSTRUCT - Instituto de I&D em Estruturas e Construções - funded by national funds through the FCT/MCTES (PIDDAC). This work was also supported through the FiberBridge – Fatigue strengthening and assessment of railway metallic bridges using fiber-reinforced polymers (POCI-01-0145-FEDER-030103) by FEDER funds through COMPETE2020 (POCI) and by national funds (PIDDAC) through the Portuguese Science Foundation (FCT/MCTES). The authors would also like to acknowledge the Institute of Construction (IC - FEUP, Portugal) and the Wroclaw University of Science and Technology (Poland).

References

Carpinteri, A., & Spagnoli, A. (2001). Multiaxial high-cycle fatigue criterion for hard metals. *International Journal of Fatigue*, *1*, 135–145.

Correia, J. A. F. O., de Jesus, A. M. P., Fernández-Canteli, A., & Calçada, R. A. B. (2015). Modelling probabilistic fatigue crack propagation rates for a mild structural steel. *Frattura Ed Integrita Strutturale*, *31*, 80–96. https://doi.org/10.3221/IGF-ESIS.31.07

Dang-van, K. (1993). Macro-Micro Approach in High-Cycle Multiaxial Fatigue. In D. L. McDowell & R. Ellis (Eds.), *Advances in MultiaxialFatigue* (pp. 120–130). Philadelphia: American Society for Testing and Materials.

Dantas, R., Correia, J. A. F. O., Lesiuk, G., Jovasevic, S., Rozumek, D., Rebelo, C., … de Jesus, A. M. P. (2019). Evaluation of biaxial (axial+torsional) high-cycle fatigue behaviour of S355 structural steel. *IRAS 2019: First International Symposium on Risk Analysis and Safety of Complex Structures and Components*, 1–2.

Dantas, Rita. (2019). *Fatigue life estimation of steel half-pipes bolted connections for onshore wind towers applications*. University of Porto.

Findley, W. N. (1958). *A theory for the effect of mean stress on fatigue of metals under combined torsion and axial load or bending*. Engineering

Materials Research Laboratory, Division of Engineering,Brown University.

Gough, H. J., & Pollard, H. V. (1935). The Strength of Metals under Combined Alternating Stresses. *Proceedings of the Institution of Mechanical Engineers*, *131*((3)), 3–103. https://doi.org/10.1243/PIME

Kamal, M., & Rahman, M. M. (2018). Advances in fatigue life modeling: A review. *Renewable and Sustainable Energy Reviews*, *82*, 940–949. https://doi.org/10.1016/j.rser.2017.09.047

Matake, T. (1977). An Explanation on Fatigue Limit under Combined Stress. *Bulletin of the JSME*, *20*(141), 257–263.

Papadopoulos, I. V. (1994). A new criterion of fatigue strength for out-of- phase bending and torsion of hard metals. *Fatigue*, *16*, 377–384.

Papadopoulos, Ioanis V., Davoli, P., Gorla, C., Filippini, M., & Bernasconi, A. (1997). A comparative study of multiaxial high-cycle fatigue criteria for metals. *International Journal of Fatigue*, *19*(3), 219–235.

Rozumek, D., & Pawliczek, R. (2004). *Opis rozwoju pęknięć i zmęczenia materiałów w ujęciu energetycznym. Wieloosiowe zmęczenie losowe elementów maszyn i konstrukcji cz. VII*. Opole: Wydawnictwo Politechniki Opolskiej.

Sadek, S., & Olsson, M. (2016). A probabilistic method for multiaxial HCF based on highly loaded regions below the threshold depth. *International Jornal of Fatigue*, *87*, 91–101. https://doi.org/10.1016/j.ijfatigue.2016.01.002

Sines, G. (1955). Failure of materials under combined repeated stresses with superimposed static stresses. *National Advisory Committee for Aeronautics*.

Sines, G. (1959). Behavior of Metals under Complex Static and Alternating Stresses. In J. L. Sines, G. and Waisman (Ed.), *Metal Fatigue* (pp. 145–169). McGraw-Hill.

Susmel, L. (2008). Multiaxial fatigue limits and material sensitivity to non-zero mean. *Fatigue & Fracture of Engineering Materials & Structures*, *31*, 295–309. https://doi.org/10.1111/j.1460-2695.2008.01228.x

Susmel, L. (2009). *Multiaxial notch fatigue: From nominal local stress/strain quantities*. Woodhead Publishing Limited.

Susmel, L., & Lazzarin, P. (2002). A bi-parametric Wöhler curve for high cycle multiaxial fatigue. *Fatigue & Fracture of Engineering Materials & Structures*, *25*, 63–78.

Susmel, L., & Tovo, R. (2011). Estimating fatigue damage under variable amplitude multiaxial. *Fatigue & Fracture of Engineering Materials & Structures*, *34*, 1053–1077. https://doi.org/10.1111/j.1460-2695.2011.01594.x

Susmel, L. (2013). On the estimation of the material fatigue properties required to perform the multiaxial fatigue assessment. *Fatigue and Fracture of Engineering Materials and Structures*, *36*, 565–585. https://doi.org/10.1111/ffe.12035

Susmel, L, Hattingh, D. G., James, M. N., & Tovo, R. (2017). Multiaxial fatigue assessment of friction stir welded tubular joints of Al 6082-T6. *International Journal of Fatigue*, *101*, 282–296. https://doi.org/10.1016/j.ijfatigue.2016.08.010

Susmel, Luca. (2010). A simple and efficient numerical algorithm to determine the orientation of the critical plane in multiaxial fatigue problems. *International Journal of Fatigue*, *32*(11), 1875–1883. https://doi.org/10.1016/j.ijfatigue.2010.05.004

Zhang, J., Shang, D., Sun, Y., & Wang, X. (2018). Multiaxial high-cycle fatigue life prediction model based on the critical plane approach considering mean stress effects. *International Jornal of Damage Mechanics*, *27*(1), 32–46. https://doi.org/10.1177/1056789516659331